Submitted for the Cluster Special Issue: 15 March, 2001

Cluster boundary-layer measurements and optical observations at magnetically conjugate sites

J. Moen[1,2], J. A. Holtet[1], A. Pedersen[1], B. Lybekk[1], K. Svenes[3], K. Oksavik[4], F. Søraas[4], M. André[5]

[1]Department of Physics, University of Oslo, P. O. Box 1048 Blindern, N-0316 Oslo, Norway.

[2]Also at Arctic Geophysics, University Courses on Svalbard, N-9170 Longyearbyen, Norway.

[3] Norwegian Defence Research Establishment, Division for Electronics, P. O. Box 25, N-2007 Kjeller, Norway.

[4]Department of Physics, University of Bergen, N-5007 Bergen, Norway.

[5]Swedish Institute of Space Physics, Uppsala Division P. O. Box 537, SE-751 21 Uppsala, Sweden

Correspondence to:

J. Moen
Department of Physics
University of Oslo
P.O.Box 1048 Blindern
N-0316 Oslo
NORWAY

E-mail: jmoen@fys.uio.no
Ph/Fx: +47 2285 5666/5671

Abstract

The Cluster spacecraft experienced several boundary-layer encounters when flying outbound from the magnetosphere to the magnetosheath in the dusk sector on January 14, 2001. The boundary layer was populated by magnetosheath electrons, but in not quite as high densities as in the magnetosheath itself. The Cluster ground track was calculated using the Tsyganenko 96 model for the magnetic field, which was found to be quite sensitive to the IMF orientation. Two of Cluster's boundary-layer encounters are associated with auroral intensifications in the 15-17 MLT sector west of Svalbard. NOAA-12 probed the auroral precipitation associated with the second encounter, and associated the discrete aurora in the 1630 MLT sector to an 10 keV electron beam poleward of the 30 keV electron-trapping boundary. A sequence of three moving auroral forms emanating from this activity region are likely candidates for flux transfer events. The auroral signatures are discussed in relation to earlier observations, and appear to be an example of the boundary plasma sheet on open field lines.

1. Introduction

Low-altitude polar orbiting satellites, combined with optical observations from the ground, have been used intensively for more than a decade as an indirect approach for determining magnetospheric boundary layer sources of auroral phenomena. Newell and Meng (1988, 1992) subdivided the "soft zone" dayside precipitation region into four different regions: the dayside extension of the boundary plasma sheet (BPS), the low-latitude boundary layer (LLBL), cusp proper, and mantle. They established an automated identification scheme to

discriminate among the four precipitation regions. Newell and Meng (1992) presented a probability map for observing the various boundary layers, where the cusp proper spans ~3 hours centred on local noon (~1030-1330 MLT). In the ionosphere the LLBL borders on the equatorward side of the cusp near noon, but extends further pre- and post-noon than the cusp (~09-15 MLT). The plasma mantle borders on the poleward side of the cusp and the LLBL. The BPS borders on the dawn and dusk end of the LLBL. The key distinction between the LLBL and the cusp is the presence of energetic magnetospheric particles in the LLBL. The BPS located poleward of the CPS are characterised by more spatially and spectrally structured electron precipitation than the CPS. The BPS also contains a dense component of accelerated magnetosheath-like ions.

Sandholt *et al.* (1998) subdivided dayside auroral activities into seven types, and tentatively associated them with the statistical precipitation map described above. Type 1 occurs in the midday sector (09-15 MLT) for southward IMF, and is dominated by the 630.0 nm emission. It includes rayed bands and quasi-periodic sequences of poleward moving auroral forms (PMAFs). Type 1 aurora comprise open LLBL, cusp, and mantle (Sandholt *et al.,* 1993; Moen *et al.,* 1998), and the moving auroral forms are believed to be footprints of flux transfer events (FTEs). Type 2 is dominated by the 630.0 nm emission, but is located at much higher latitudes than type 1. Type 2 is stimulated by magnetosheath electrons injected by lobe reconnection for northward IMF (Øieroset *et al.,* 1997). Type 3 is a diffuse glow of 557.7 nm, and is located equatorward of type 1 with an emission gap between. It is attributed to pitch angle scattered energetic electrons from the CPS (Lorentzen *et al.,* 1996; Moen *et al.,* 1998). Types 4 and 6 are discrete forms in the prenoon sector (06-09 MLT), strong in both the 557.7 and 630.0 nm. They are

attributed to BPS origin (Ober *et al.,* 2000; Farrugia *et al.,* 2000; Lorentzen and Moen, 2000). Type 4 occur as multiple forms for IMF B_Z north, and type 6 often appear as longitudinal extension of the type 1 activity at dawn. Types 5 and 7 are discrete forms in the dusk sector (15-18 MLT) containing strong red and green line emissions. Type 5 appears as multiple arcs for IMF B_Z north, and type 7 appears as an extension of the type 1 auroral activity during IMF B_Z south. The main difference, therefore, between type 1 and type 7 is the increase of the green line intensity.

It must be noted that Newell and Meng (1988) based their identification scheme on quantitative criteria rather than physical arguments. Model simulations have shown that open LLBL, cusp, and mantle are different stages of the evolution of a newly reconnected flux convecting away from the merging site. It is now accepted that the LLBL may be entirely on open field lines (Lockwood and Moen, 1996; Moen *et al.,* 1996; Lockwood *et al.,* 1998), but the BPS is usually thought of being definitely on closed field lines. However, this view may have to be revised. Sometimes the energy-dispersed ion signature, interpreted as a reconnection signature, begins in the BPS (Lockwood *et al.,* 1997), and Milan et al. (2000) presented UVI images and HF radar observations suggesting that PMAFs can be seven hours of MLT in length and extend as far as 19 MLT.

In this paper we present two auroral events in the 15-17 MLT sector west of Svalbard, which appear magnetically conjugate with high-altitude Cluster observations. Conjunction was obtained when Cluster encountered boundary layer plasma in the dusk sector on January 14, 2001. We will demonstrate use of the Tsyganenko 96 model (Tsyganenko and Stern, 1996) to identify magnetic conjugacy between the Cluster spacecraft and the auroral ionosphere, noting that

conjugacy is sensitive to solar wind conditions and has associated uncertainties. The postnoon auroral activity investigated here is classified as the type 7 activity mentioned above, and is discussed with respect to the open/closed field line controversy for the BPS. Available Cluster data for this study are electron particle data from the PEACE instrument, spacecraft potential, and electric field measurements from the EFW instrument

2. Instrumentation

Each Cluster spacecraft carries an electric field and wave experiment (EFW). This experiment measures the potential difference between two perpendicular axes of double probes; the spherical probes are mounted at the tips of four radial booms 44 m in length. Each probe is electronically controlled to be close to its local plasma potential where a resistive coupling to the plasma is optimised for reliable measurements. Initial calculations in the solar wind, when compared with measured ion drift speeds, have demonstrated accuracies to a fraction of one mV/m. The electric field experiment provides information about the electric field components E_X (GSE) and E_Y (GSE), and from the assumption $\mathbf{E}\cdot\mathbf{B} = 0$ it is possible to calculate E_Z. In combination with three magnetic field components it is then possible to calculate $\mathbf{E}x\mathbf{B}/B^2$, the plasma transport perpendicular to **B**. The electric field probes are electronically controlled to be 0.5 to 1.0 V positive relative to the ambient plasma and can serve as a reference for the spacecraft potential, which in turn can be calibrated to provide information about electron density. More details are given in Gustafsson et al. (this issue).

The PEACE (Plasma Electron and Current Experiment) instrument is a dual sensor system designed to measure the three-dimensional velocity distribution of

electrons in the energy range from 0.6 eV to 27 keV, and to detect electrons arriving from all pitch angles. The instrument consists of a data processing unit and two sensors. The sensors are hemispherical electrostatic energy analysers with position-sensitive micro-channel plate detectors. Each sensor is mounted on the spacecraft so as to observe a 180^o field of view in the plane defined by the spacecraft spin axis and the radial direction in the spin plane. The two sensors, LEEA and HEEA (High and Low Energy Electron Analysers), are mounted on opposite sides of the spacecraft so that they have a combined instantaneous field of view of 360^o. In normal operations, the sensors operate at a rate of 32 sweeps in each four-second satellite spin. LEEA covers the range up to about 1000 eV, and HEEA covers the range from about 40 eV to about 27 keV. Technically, either sensor can cover the full energy range, although in certain environments the difference in geometric factor means that one or the other sensor is preferred to cover particular energy ranges. The reader is referred to Johnstone *et al.* (1997) for a full description of the instrument.

NOAA-12 is a low-altitude polar orbiting satellite operating at an altitude of ~820 km above the Earth's surface. The NOAA satellites carry two complements of particle instruments, the Total Energy Detector (TED) and the Medium Energy Proton and Electron Detector (MEPED). TED measures electrons and ions between 0.3 and 20 keV, in two viewing directions, one toward zenith and the other 30^o to zenith. This instrument has been designed to obtain the energy flux moment, but also provides crude electron and ion energy spectra as well. MEPED consists of solid-state detector telescopes, one pointing toward zenith to view particles that precipitate into the ionosphere, the other at 90^o to zenith to view particles that will magnetically mirror above the atmosphere. The energy ranges sensed are for

electrons >30 keV, >100 keV, >300 keV, all with a 1000 keV maximum energy, and for ions 30-80 keV, 80-250 keV, 250-800 keV, 800-2500 keV and >2500 keV. MEPED provides information on energetic magnetospheric particle fluxes (>30 keV) and helps locate the electron trapping boundary.

The auroral activity was surveyed by an all-sky imager (ASI) located at Ny-Ålesund (78.9^{o} N, 11.9^{o} E, 76.07^{o} CGMLAT). The Tsyganenko 96 magnetic field model (T96) is used to connect the Cluster in-situ measurements to the ground-optical observations.

3. Observations

Figure 1 illustrates the location of Cluster above the northern hemisphere on January 14, 2001, viewed in a GSE XZ plane in the left panel and in a GSE YZ plane on the right. The spacecraft number 1, SC1, like all the other three (SC2-SC4) were at GSE position (2.72, 8.03, 9.13) R_E at 1230 UT. The red curve in each panel marks the orbital path travelled from 1230 to 1400 UT. Direction of movement is indicated by an arrow. The Cluster satellites moved radially out in the dusk sector when collecting the data to be presented. The figure was made using the orbit visualization tool for Cluster (http://ovt.irfu.se) employing the T96 model for the magnetic field.

Figure 2 presents observations from the PEACE and from EFW experiments on spacecraft 1 (SC1) from 1230 to 1530 UT. The top panel shows a colour-coded electron spectrogram from PEACE, where accumulated counts (for LEEA) are plotted versus energy and time. At first glance we see that the spacecraft alternated between two distinct plasma populations, that is, high-density soft electrons (30-200 eV), and low-density energetic electrons that can be glimpsed at the highest energy

ranges. The absence of the soft energy at the beginning tells us that the spacecraft initially was inside the magnetopause, where the measurements are dominated by the energetic (E > 1 keV) particles usually encountered on closed field-lines. Between 1252 and 1515 UT it had several encounters with a soft electron population; the first one lasted ~4 minutes, and the most extensive one lasted from 1327 and 1357 UT. These two encounters will be related to auroral activity observed between Svalbard and Greenland. Notably, the high-energy component disappears at every excursion into the soft electron regime. At 1515 UT, the spacecraft had definitely reached the magnetosheath.

The second panel from the top in Figure 2 shows the negative of the spacecraft potential with an electron density scale on the right side. This way of plotting the spacecraft potential means that increasing electron density is upwards. This parameter has periodic excursions between –20 V and –25 V in the tenuous magnetospheric plasma. This periodic variation is caused by short operations of the plasma resonance sounder Whisper on Cluster. The upper trace corresponds to the N_e scale on the right of this panel.

Comparing spacecraft potential with PEACE electron data, it is evident that spacecraft potential is a useful parameter for locating boundary-layer crossings between low- and high-density plasma populations. After 1515 UT, when the satellite has entered the magnetosheath, the negative of the plasma potential reaches a quasi-steady level of –5 V. The two boundary-layer excursions that will be linked to auroral activity enhancements west of Svalbard are annotated BL-E1 and BL-E2, meaning boundary-layer event 1 and 2. The density associated with BL-E1 is significantly lower than that for BL-E2, and the corresponding spacecraft potential is around –14 V and –7 V, respectively.

The electric field components E_X (GSE) and E_Y (GSE) are given in the following two panels of Figure 2, and we will use these values for justifying **E**x**B** drift of the plasma associated with BL-E1.

Figure 3 presents a sequence of 630.0 nm all-sky images from 1251 to 1256 UT, that is, covering the time interval when Cluster encountered BL-E1 above. The raw images have been cut at 75 degrees zenith angle and projected onto a map assuming an altitude of 250 km for the 630.0 nm emission. The acquisition time is given at the top of each frame. The curved line in yellow represents the Cluster ground-track from 1020 UT until it went out of the field of view over Greenland around 1320 UT. The T96 model of the magnetic field was used for the field line tracing, with driving parameters B_X = -4nT, B_Y=-2 nT, B_Z=0 nT, solar wind dynamic pressure 1.2 nPa, and Dst = -2. Cluster's position along the ground track is marked with a white square at 20 min intervals in the top left frame. In the subsequent frames the calculated position corresponding to the time the picture was taken has been marked. In the top left frame at 1251 UT, we see two arc filaments between Greenland and Svalbard, located poleward of the Cluster path. At ~1253 UT, a third form brightened near eastern Greenland. This form intruded in the field of view in a region equatorward of where the other two subsequently faded, 1254.10-1255.30 UT. This third form reached the Cluster footprint between 1252 and 1253 UT, nearly coincident in time with the in-situ measurement of BL-E1. The auroral form expanded further eastward, and retreated poleward from 1255 UT. At 1256.30 UT, the footprint of Cluster was at the equatorward edge of the auroral transient, nicely corresponding with Cluster leaving BL-E1 (Figure 2).

Figure 4 is a sequence of all-sky images demonstrating the auroral activity to be discussed in relation to Cluster's boundary-layer excursion BL-E2 from 1327-1357 UT. The yellow ground track of Cluster was obtained by using B_X = -2nT, B_Y= 4 nT, B_Z=0 nT, solar wind dynamic pressure 1.2 nPa, and Dst = -2 as input in T96. The red trajectory is the one we used for the previous case in Figure 3. The difference between the two will be commented on in the discussion. At the event onset, Cluster had already moved out of the field of view over Greenland. In Figure 4 we see an initial brightening above eastern Greenland around 1331 UT. This activity expanded rapidly toward Svalbard. Between 1341.30 and 1344.10 UT, an auroral form detached from the main activity region and propagated east towards Heiss Island. NOAA-12 traversed the quasi-persistent auroral arc between 1348 and 1349 UT, as illustrated in the two right-hand frames in the bottom row in Figure 4. The satellite flew along the straight red line from south-east to north-west. Electron particle data sampled along this trajectory are presented in Figure 5. The solid curves in the three upper panels represent precipitating electrons at given energies, whilst the dot-dashed curves in the second and third panels represent fluxes perpendicular to the magnetic field. NOAA-12 crossed northbound through the 30 keV electron-trapping boundary at 1348 UT indicated by the vertical line. North of the electron-trapping boundary there is a belt of structured 0.3-0.46 keV electrons precipitation. At ~1348.30 UT the electron energy flux peaked at 10 ergs cm^2 s^{-1}, which corresponds to the intersection of the bright arc. The characteristic energy associated with this distinct peak in energy flux is 10 keV. The eastward-moving form breaking off from the quasi-persistent background arc, as described above, was followed by two similar ones that tore off the background arc at ~1351 and

~1353 UT. Then the auroral activity ceased, and the background arc faded at the time Cluster went out of BL-E2 at 1357 UT.

4. Discussion

4.1 Solar wind conditions

ACE measured a solar wind bulk speed of ~380 kms^{-1}, corresponding to an advection time of about one hour between the position of ACE at ~230 R_E upstream and the Earth's magnetopause. ACE observed a significant northward turning around 0945 UT from IMF B_Z (GSE) of –4 nT to +4 nT. From 0945 to 1340 UT, B_Z was predominantly positive. B_Z fluctuated between zero and + 4 nT, but with brief negative excursions around 1045 UT (-0.5 nT), 1150 UT (-0.5 nT), 1230 UT (-0.5 nT), and 1240 UT (-2 nT). B_X varied between 0 and –5 nT, and B_Y from –4 to 4 nT. Assuming a time lag of ~1 hour between ACE and Cluster observations, the two cases where Cluster entered the boundary layers at 1251 and 1330 UT are tentatively related to the negative B_Z bays at 1150 and 1230 UT, respectively. IMF B_X was –4 nT and B_Y was –2 nT for the first case, and IMF B_X was –2.5 nT and B_Y was +4 nT for the second case. The $-B_X$ dominance on a weakly southerly IMF favours opening of magnetic flux near the southern hemisphere cusp. It is therefore not likely that Cluster was close to a merging location during the two boundary-layer encounters studied here.

4.2 Field-aligned mapping and magnetic conjugate measurements

Mapping along magnetic field lines from the outer magnetosphere to the ground is a non-trivial task involving uncertainties. The red and the yellow curves in the upper left frame in Figure 4 illustrate an ~80 km latitudinal shift southward of the

Cluster ground trajectory when changing from -4nT to –2 nT in B_X and from -2 nT to +4nT in B_Y. Ober *et al.* (2000) demonstrated a similar displacement for a Polar pass over Svalbard. In order to obtain a quantitative agreement between electron fluxes observed by Polar, and the resulting auroral emissions in the ionosphere, they shifted the footprint trajectory by adjusting the dynamic pressure input to the model. That is, they used dynamic pressure as a free parameter to obtain good correspondence between electron precipitation fluxes and auroral activity. For the two situations presented here, when the aurora was far off zenith of the optical site, a quantitative comparison between variations in auroral intensity and spectral content, with variations in field-aligned electron fluxes and energy, is not recommended. Therefore we used the measured solar wind conditions as driving parameters.

The red curve in Figure 4 is exactly the same as the yellow curve in Figure 3. The mapping in Figure 3 ties the boundary layer crossing BL-E1 very convincingly to the crossing of the discrete postnoon auroral form. The mapping in Figure 4 is impossible to judge, as the Cluster footprint was west of the all-sky field of view. However, the auroral activity enhancement between Greenland and Svalbard coincided in time with Cluster's encounter of BL-E2 in Figure 4, which is indicative of a close relationship between the two phenomena. This view will be strengthened further in Section 4.4, where we conclude that the auroral activity shown in Figure 4 is reconnection-related and is located on open flux.

4.3 Boundary-layer crossings and plasma movement

We conclude from Figure 3 that Cluster was initially in the magnetopshere at 1230 UT and had definitely crossed the magnetopause by 1515 UT. In between

these two extremes, Cluster had several encounters with a boundary layer populated by a magnetosheath plasma component, but of not quite as high densities as in the magnetosheath itself. During the first encounter, from 1252-1256 UT, the characteristic energy ranged from 50 to 60 eV. The density varied between 3-6 cm^{-3}, which is an increase of about an order of magnitude higher than in the magnetosphere. This increase is indicative of the spacecraft having come close to the magnetopause during this period, which is further supported by the fact that the magnetic clock angle increased by at least 30^o during the same period. Hence, it is reasonable to assume that the spacecraft entered the magnetosheath boundary layer during this time. The spacecraft then returned back into the magnetosphere, as shown by the return of the energetic electron population (also consistent with RAPID observations). The magnetic field (not presented) was almost directly in the –Y (GSE) direction. At 1252 UT the electron density increased, but not quite to magnetosheath values, and then dropped again at 1256 UT. In this interval electrons of typical magnetosheath energies were observed. This looks like an inward and an outward movement of the magnetopause influencing the boundary layer. The electric field components E_X (GSE) and E_Y (GSE) are given in the two bottom panels in Figure 2. Because the magnetic field (**B**) was nearly directed along –Y direction at 1252, E_Z (GSE) must be zero and the **E**x**B** velocity is in the –Z direction and has a magnitude of $E_X/B_Y = 50$ kms^{-1}, which means an inward movement of the ambient plasma. In the middle of this density enhancement B_Z increased to approximately 8 nT, and correspondingly the **E**x**B** velocity shifts to –Z and X direction, with a magnitude of about 100 kms^{-1}. At 1256 UT **B** is again in -Y direction, but E_X has turned to –1 mVm^{-1}, and the **E**x**B** velocity is in the Z-direction, which indicates an outward movement.

At 1327 UT SC-1 made another crossing out of the magnetosphere, again marked by the disappearance of high-energy electrons and the occurrence of a colder and denser population. This population is characterised by energies in the range 50 - 80 eV and densities of 20-40 cm^{-3}. Note that in a short interval between 1330 and 1332 UT, N_e increases to magnetosheath values (marked MSh in Figure 2). B_Z increased to 20 nT, and the **E**x**B** velocity increased to 125 kms^{-1} in –X and +Y direction, which is the expected direction and velocity in the magnetosheath. This is therefore a clear crossing of the magnetospause. The spacecraft returned to a less dense plasma (BL-E2), presumably inside the magnetopause. The satellite remained in this environment until 1357 UT when it again returned into the magnetosphere, as seen by the reappearance of the high-energy electrons. It is interesting to observe that for the MSh interval 1330 to 1332 UT, electron energy was nearly identical to that observed deeper in the magnetosheath at 1510 UT. In the interval 1340-1343 UT (inside the magnetospause) the electron energy was higher (increase from a 25-75 eV range to a 35-120 eV range) This period very likely represented a crossing of the outer cusp region (around 13 R_E). It turned out to consist of a fairly structured electron population with irregular density variations, but a general increase towards higher energies during the crossing.

4.4 NOAA-particle data and auroral morphology

NOAA-12 cut through the east end of the auroral activity that surged into the field of view from the west and reached Svalbard around 1341 UT (see Figure 4). It passed the 30 keV electron trapping boundary marked by the vertical line in Figure 5 at 1347.45 UT. By inspecting the red satellite path in the 1348.10 UT frame of Figure 4, we can see that the satellite was then at a position well south of the bright

arc (~250 km). Sometimes a drizzle of energetic electrons occurs south of the electron-trapping boundary giving rise to a 557.7 nm glow aurora (Moen *et al.*, 1998), termed type 3 aurora by Sandholt *et al.* (1998) (cf. the introduction). That was not observed here, but we can see some precipitating high-energy electrons around 1346 UT (the solid curve in the second and third panel in Figure 5). Poleward of the electron-trapping boundary, a significant flux of 0.3-0-46 keV electrons was observed between 1347.45-1350 UT, likely of magnetosheath origin, and it gave rise to the faint 630.0 nm luminosity seen at either side of the bright arc. The most significant energy flux peaking at 10 ergs/(cm^2 s), corresponding to the bright arc, was not spectrally resolved by NOAA-12. However, the characteristic energy of several keV indicates that the precipitating electrons had been through a potential drop, and that the arc is representing an upward field-aligned current sheet. In the light of accumulated knowledge from DMSP observations, the region of electron beams of several keV, mixed with a soft component in this time sector (1630 MLT), is what traditionally is classed as BPS precipitation (cf. introduction).

Another very interesting feature of the auroral activity observed in Figure 4 is the sequence of moving auroral forms detaching from the quasi-persistent background arc. At ~1342 UT the first form in the sequence separated from the background aurora between Greenland and Svalbard and subsequently drifted eastward. This moving auroral form was followed by two similar ones that separated from the active region at ~1351 and ~1353 UT, after which all the activity faded. The category of moving auroral forms is taken as a candidate signature of flux transfer events (FTEs; e.g. Sandholt *et al.*, 1993 and Moen *et al.*, 1995). This is the type auroral activity that Sandholt *et al.* (1998) named type 7 (cf. introduction). They attributed type 7 to BPS origin, but pointed out that the type 7 activity appears

to be an extension of postnoon type 1 aurora (open LLBL/cusp/mantle and reconnection signatures). BPS are sometimes associated with energy-dispersed ions, and Lockwood (1998) suggested that BPS sometimes may be on open field lines. Milan *et al.* (2000) attributed a discrete Polar UVI arc extending into the 19 MLT sector to a reconnection X-line. Poleward-moving forms emanated from this arc in the 14-16 MLT sector, very similar to what we have reported here.

As the east end of the auroral activity was on open field lines and showed key features of magnetic reconnection, it is quite reasonable that the activity extended towards noon (Milan *et al.,* 2000), and hence was related to the boundary-layer encounter BL-E2 by Cluster further west. In section 4.3 above we concluded that Cluster was visiting the outer cusp associated with this event. The Cluster and the NOAA-12 observations are not directly comparable, as their ionospheric footprints were separated by more than 2 hours in MLT. Nevertheless, the case presented here strengthens the view that open BPS sometimes can be an extension of cusp into the dusk sector.

Now let us go to Cluster's intersection of the discrete arc presented in Figure 3. The ray bundles seen in the upper row of images in Figure 3 are typical signatures of type 1 cusp auroral activity (Sandholt *et al.,* 1998). The absence of energetic electrons during this encounter (BL-E1) indicates open field lines. The eastward limit of the auroral activity was near Svalbard and did not extend further into the evening sector. Hence, it is reasonable to conclude that BL-E1 and the associated auroral form were related to dayside boundary dynamics. The auroral activity was discrete in nature and contained a signifficant 557.7 nm component (data not presented), which puts it in the category of Type 7 aurora. The 557.7 nm component

indicates that some process has accelerated the auroral electrons on their way down from the magnetosheath source region.

5. Summary and concluding remarks

We have related two boundary layer events observed by Cluster to intensifications in auroral activity between Greenland and Svalbard. We have demonstrated use of the T96 model to identify the Cluster footprint in the ionosphere. The mapping is quite sensitive to solar wind conditions.

The auroral activity was observed in the 15-17 MLT sector and was of type 7, traditionally ascribed to BPS origin. The Cluster as well as the NOAA-12 particle measurements indicate that this activity is on entirely open field lines.

The spacecraft potential is a key parameter for accurately defining boundary layer crossings. The spacecraft potential measurements have a time resolution of better than 0.1 s, and using data from the constellation of all four satellites, it is possible to get an approximate picture of boundary surface orientation and movement. A high time resolution plot of the potential on all four spacecraft during the encounter of the BL-E1 structure (Figure 6) shows that the spacecraft traverses the leading flank of the boundary layer event in the order SC2, SC3, SC1 and SC4. The same order is maintained when the spacecraft are leaving the boundary layer event. This indicates that an inward bulge of the magnetopause that propagated tailward over the satellites caused the inbound and outbound encounters.

We will encourage a more detailed study on BL-E1 and BL-E2 including the ion particle data and the magnetic field experiments onboard the Cluster satellites to explore further whether or not Cluster was in contact with merging field lines.

Acknowledgements:

The Norwegian Research Council has funded the Norwegian participation in the Cluster mission. This work has also benefited from the AFOSR grant F61775-01-WE014. We wish to acknowledge N. Ness at Bartal Research Institute and CDAWeb for distribution of ACE key parameter. We also acknowledge the use of Cluster magnetic field data for obtaining an approximate direction of the magnetic field and for calculating approximate $\mathbf{E}x\mathbf{B}/B^2$ values. Thanks to K. Stasiewicz and co-workers who have developed the orbit visualisation tool for Cluster.

References

Farrugia, C. J., P. E. Sandholt, N. C. Maynard, W. J. Burke, J. D. Scudder, D. M. Ober, J. Moen, and C. T. Russell, Pulsating mid-morning auroral arcs, filamentation of a mixing region in a flank boundary layer, and ULF ULF waves observed during a POLAR-Svalbard conjunction, *J. Geophys. Res., 105*, 27531-27554, 2000.

Gustaffson et al., First results of electric field and density observations by Cluster EFW based on initial amounts of operations, *Annales Geophysicae*, this issue.

Johnstone, A.D., C. Alsop, S. Burge, P. J. Carter, A. J. Coates, A. J. Coker, A. N. Fazakerley, M. Grande, R. A. Gowen, C. Gurgiolo, B. K. Hancock, B. Narheim, A. Preece, P. H. Sheather, J. D. Winningham, and R. D. Woodliffe, PEACE: a plasma electron and current instrument, *Space Sci Rev, 79*, 351-398, 1997. Reprinted in Escoubet, C.P., Russell, C.T. and Schmidt, R. (Editors), The Cluster and Phoenix missions, *Kluwer Academic Press, Dordrecht*, 1997.

Lockwood, M., Identifying the open-closed field line boundary, in *Polar Cap Boundary Phenomena* by J. Moen et al., (eds.), NATO Advanced Study Institute Series, *Kluwer Academic Press, Dordrecht, Vol. 509,* 415-432, 1998.

Lockwood, M., and J. Moen, Ion populations on open field lines within the low-latitude boundary layer: theory and observations during a dayside transient event, *Geophys. Res. Lett., 23*, 2895-2898, 1996.

Lockwood., M., S. Fuselier, A.D.M. Walker, and F. Søraas, A summary of the NATO ASI on polar cap boundary phenomena, in *Polar Cap Boundary Phenomena* by J. Moen et al., (eds.), NATO Advanced Study Institute Series, *Kluwer Academic Press, Dordrecht, Vol. 509,* 415-432, 1998.

Lorentzen, D. A., C. S. Deehr, J. I. Minow, R. W. Smith, H. C. Stenbaek-Nielsen, F. Sigernes, R. L. Arnoldy, and K. Lynch, SCIFER-Dayside auroral signatures of magnetospheric energetic electrons, *Geophys. Res. Lett., 23*, 1885-1888, 1996.

Lorentzen, D. A., and J. Moen, Auroral proton and electron signatures in the dayside aurora, *J. Geophys. Res., 105*, 12733-12745, 2000.

Milan, S. E., M. Lester, S. W. H. Cowley, and M. Brittnacher, Convection and auroral response to a southward turning of the IMF: Polar UVI, CUTLASS, and IMAGE signatures of transient magnetic flux transfer at the magnetopause, *J. Geophys. Res., 105*, 15741-15755, 2000.

Moen, J., P. E. Sandholt, M. Lockwood, W. F. Denig, U. P. Løvhaug, B. Lybekk, A. Egeland, D. Opsvik, and E. Friis-Christensen, Events of enhanced convection and related dayside auroral activity, *J. Geophys. Res., 100*, 23, 917-23,934, 1995.

Moen, J., D. Evans, H. C. Carlson, and M. Lockwood, Dayside moving auroral transients related to LLBL dynamics, *Geophys. Res. Lett., 23*, 3247-3250, 1996.

Moen, J., D. A. Lorentzen, F. Sigernes, Dayside moving auroral forms and bursty proton auroral events in relation to particle boundaries observed by NOAA-12, *J. Geophys. Res., 103*, 14855-14863, 1998.

Newell, P.T., and C.-I. Meng, The cusp and the cleft/boundary layer: low-altitude identification and statistical local time variation, *J. Geophys. Res., 93*, 14,549-14,556, 1988.

Newell P.T. and C.-I. Meng, Mapping the dayside ionosphere to the magnetosphere according to particle precipitation characteristics, *Geophys. Res. Lett., 19*, 609-612, 1992.

Ober, D. M., N. C. Maynard, W. J. Burke, J. Moen, A. Egeland, P. E. Sandholt, C. J. Farrugia, E. J. Weber, J. D. Scudder, Mapping of ionospheric auroral features associated with the prenoon boundary layer to the magnetosphere, *J. Geophys. Res., 105*, 27519-27530, 2000

Sandholt, P.E., J. Moen, A. Rudland, D. Opsvik, W.F. Denig, and T. Hansen, Auroral event sequences at the dayside polar cap boundary for positive and negative IMF B_Y, *J. Geophys. Res., 98*, 7737-7755, 1993.

Sandholt, P.E., C.J. Farrugia, J. Moen, Ø. Noraberg, B. Lybekk, T. Sten, and T.L. Hansen, A classification of dayside auroral forms and activities as a function of IMF orientation, *J. Geophys. Res.,103,* 23,325-23,345, 1998.

Tsyganenko, N. A., and D. P. Stern, Modelling the global magnetic field of large-scale Birkeland current systems, *J. Geophys. Res., 101*, 27187, 1996.

Øieroset, M., P.E. Sandholt, W. F. Denig, S. W. H. Cowley, Northward interplanetary magnetic field cusp aurora and high-latitude magnetopause reconnection, *J. Geophys. Res., 102*, 11349-11362, 1997.

Figure captions:

Figure 1 An illustration of the flight path (in red) of Cluster from 1230 to 14 UT in a GSE XZ and YZ plane. Cluster moved radially outward in the dusk sector for the actual time interval.

Figure 2 The top panel shows the spectrogram obtained by PEACE at SC1 from 1230-1530 UT. The accumulated counts in each energy bin (for LEEA) have been plotted as a function of time (colour bar on right side). The second panel from the top represents the negative of the spacecraft potential for SC1. The spacecraft potential has been calibrated against electron density, and the electron density scale is given on the right. The two bottom panels show the GSE X and Y components of the electric field versus time.

Figure 3 A sequence of digital all-sky images of the 630.0 nm emission taken at Ny-Ålesund displayed on a geographical frame of reference. The auroral emission is mapped to an Earth-centred sphere at 250 km. Time is given at the top of each frame. The colour scale is linear with increasing intensity from blue to red. The yellow curve represents Cluster's groundtrack. The sequence corresponds to Cluster's boundary-layer encounter BL-E1.

Figure 4 An all-sky sequence for Cluster event BL-E2 presented in the same format as Figure 3. The red curve in the upper left frame is the Cluster trajectory calculated for Figure 3, whilst the yellow curve is the one calculated for this actual image sequence. The straight red line west of Svalbard in the 1348.10 and 1349.10 UT frames (bottom row) depicts the flight path of NOAA-12.

Figure 5 NOAA-12 electron particle observations along the path indicated by the straight red line west of Svalbard in the 1348.10 and 1349.10 UT frames in Figure 4 (bottom row). The upper panel shows the integral of down-coming electrons over the energy range 0.30-0.46 keV. The second and third panels from the top represent the integral flux over 30-1000 keV and 100-1000 keV for electrons. The solid line is the flux measured along the zenith direction, and the dot-dashed line is the flux perpendicular to that. The two bottom panels give characteristic energy and energy flux for the electron precipitation.

Figure 6 High time resolution plots of the negative of the spacecraft potential of the four Cluster spacecraft during the BL-E1 encounter. The data points represent 1 sec averages. The scale of the potential of Spacecraft 2 has been adjusted to be on the same level as the other three. Due to an unscheduled high beam current in the EDI experiment, this spacecraft was shifted to a lower potential. The periodic dips in the potential are due to operation of the Whisper sounder.

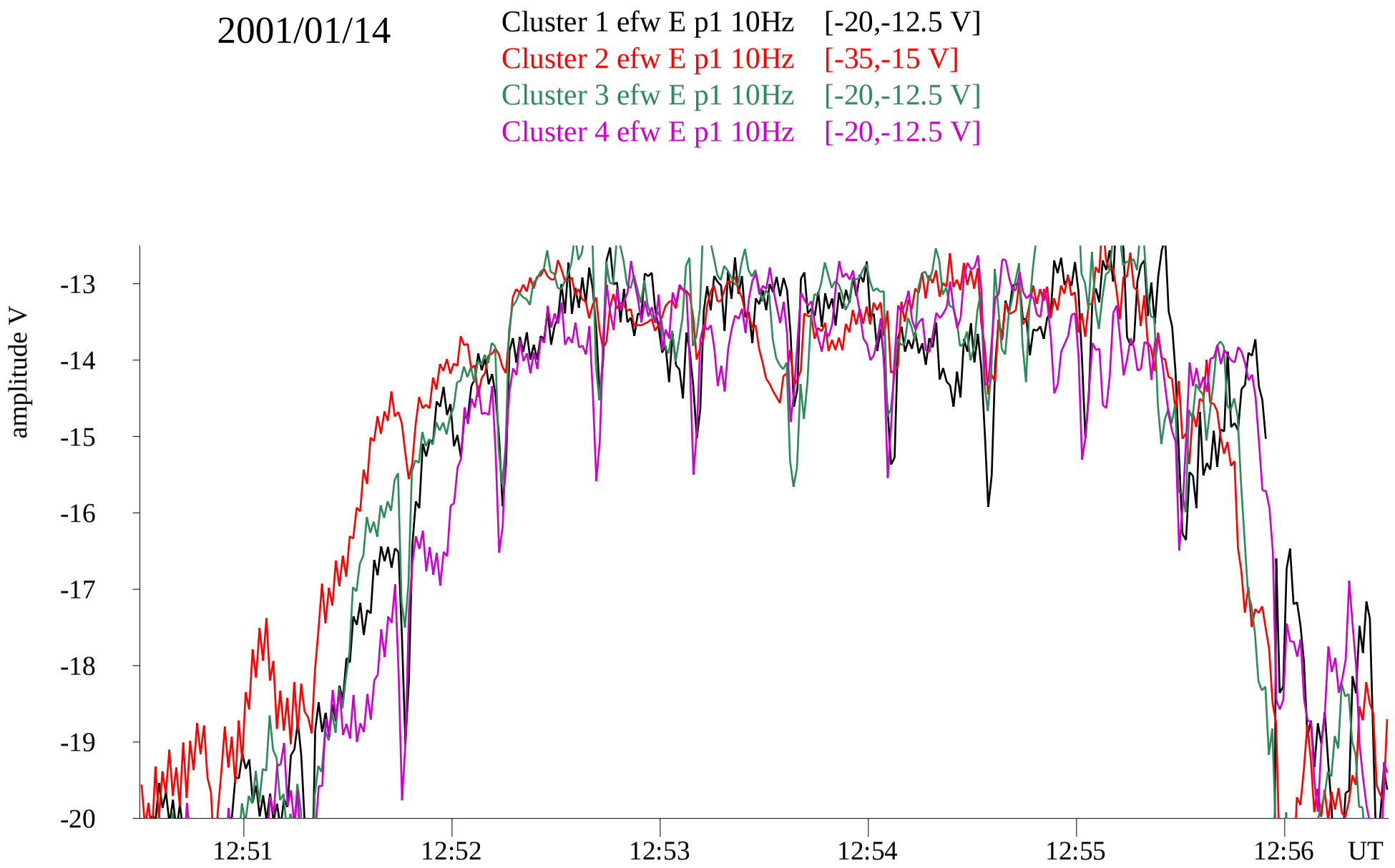
2001/01/14
Cluster 1 efw E p1 10Hz [-20,-12.5 V]
Cluster 2 efw E p1 10Hz [-35,-15 V]
Cluster 3 efw E p1 10Hz [-20,-12.5 V]
Cluster 4 efw E p1 10Hz [-20,-12.5 V]
amplitude V
-13
-14
-15
-16
-17
-18
-19
-20
12:51
12:52
12:53
12:54
12:55
12:56
UT

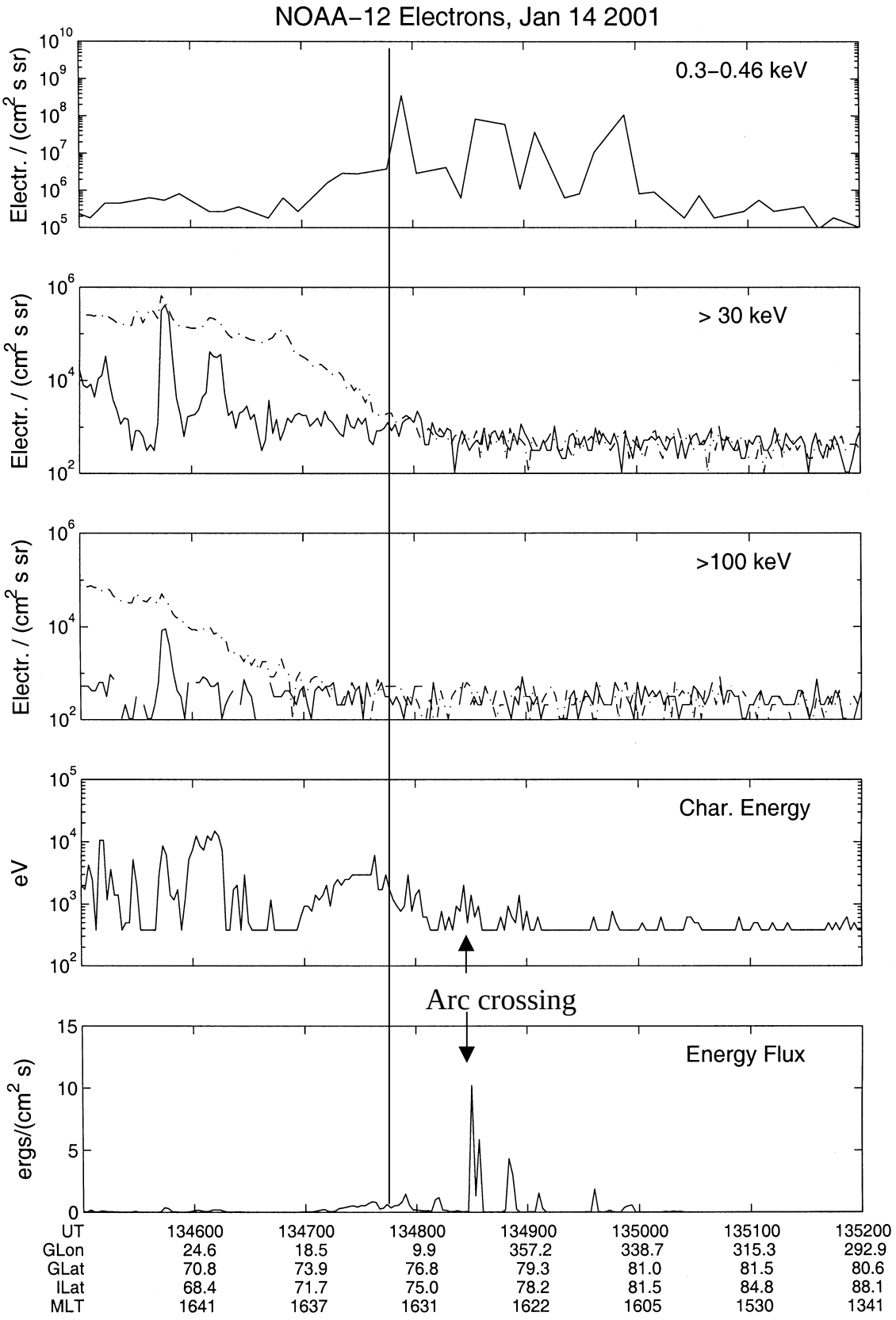
NOAA−12 Electrons, Jan 14 2001
0.3−0.46 keV
> 30 keV
>100 keV
Char. Energy
Energy Flux
Electr. / (cm² s sr)
eV
ergs/(cm² s)
Arc crossing
UT 134600 134700 134800 134900 135000 135100 135200
GLon 24.6 18.5 9.9 357.2 338.7 315.3 292.9
GLat 70.8 73.9 76.8 79.3 81.0 81.5 80.6
ILat 68.4 71.7 75.0 78.2 81.5 84.8 88.1
MLT 1641 1637 1631 1622 1605 1530 1341

Figure 5

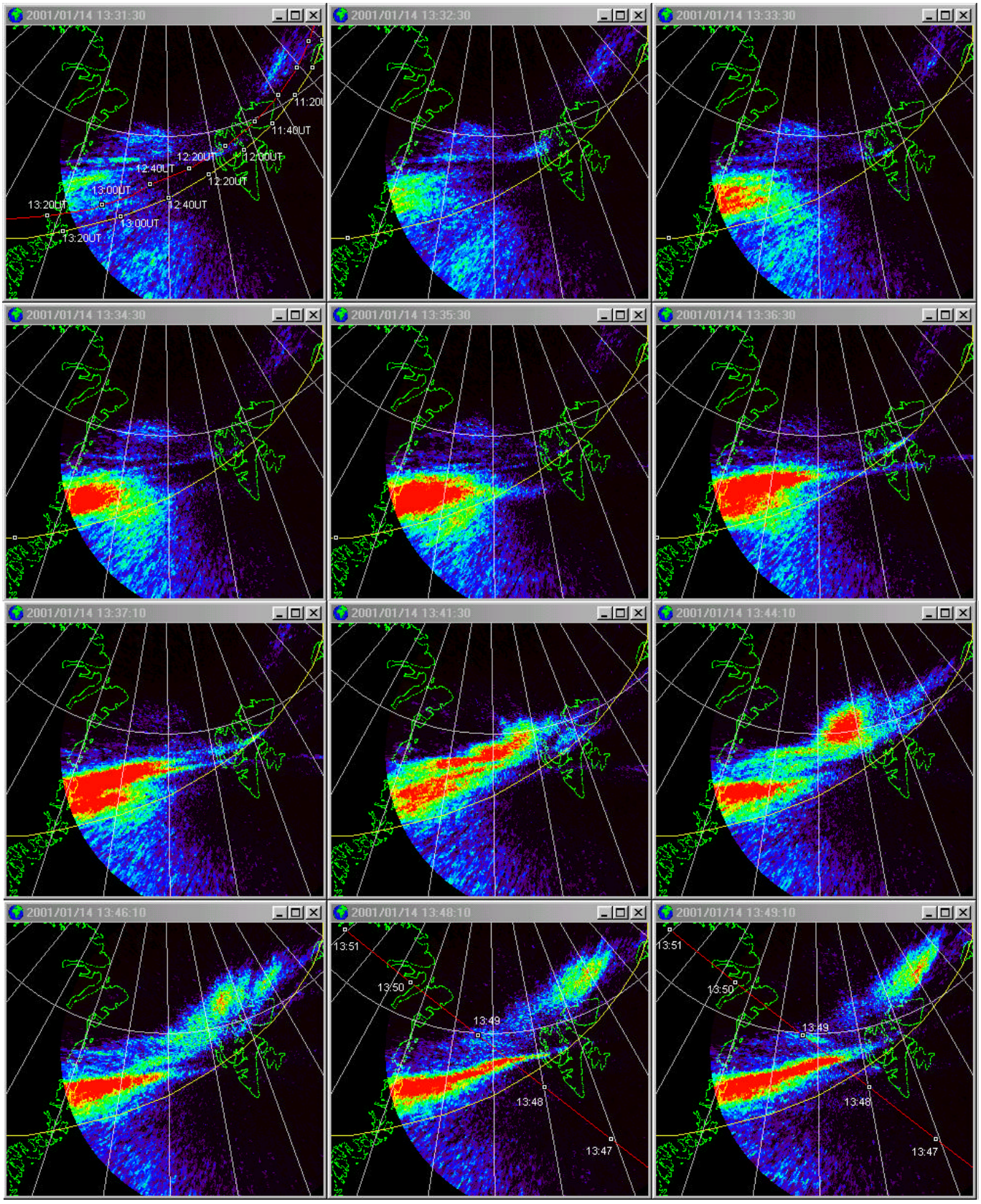
2001/01/14 13:31:30
11:40UT
12:20UT
12:00UT
12:40UT
12:20UT
13:00UT
13:20UT
12:40UT
13:00UT
13:20UT
2001/01/14 13:32:30
2001/01/14 13:33:30
2001/01/14 13:34:30
2001/01/14 13:35:30
2001/01/14 13:36:30
2001/01/14 13:37:10
2001/01/14 13:41:30
2001/01/14 13:44:10
2001/01/14 13:46:10
2001/01/14 13:48:10
13:51
13:50
13:49
13:48
13:47
2001/01/14 13:49:10
13:51
13:50
13:49
13:48
13:47

Figure 4

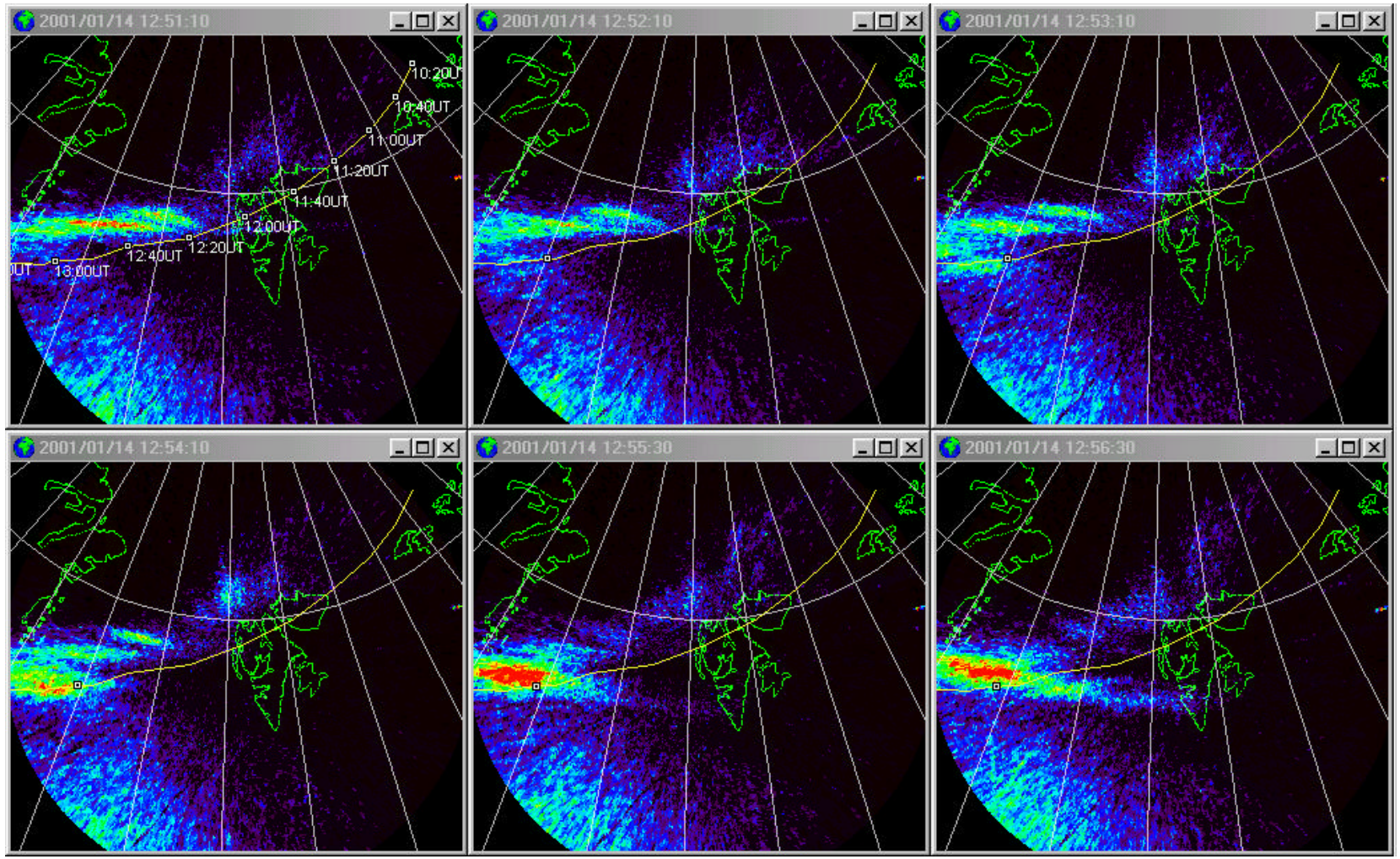
2001/01/14 12:51:10
10:20UT
10:40UT
11:00UT
11:20UT
11:40UT
12:00UT
12:20UT
12:40UT
13:00UT
2001/01/14 12:52:10
2001/01/14 12:53:10
2001/01/14 12:54:10
2001/01/14 12:55:30
2001/01/14 12:56:30

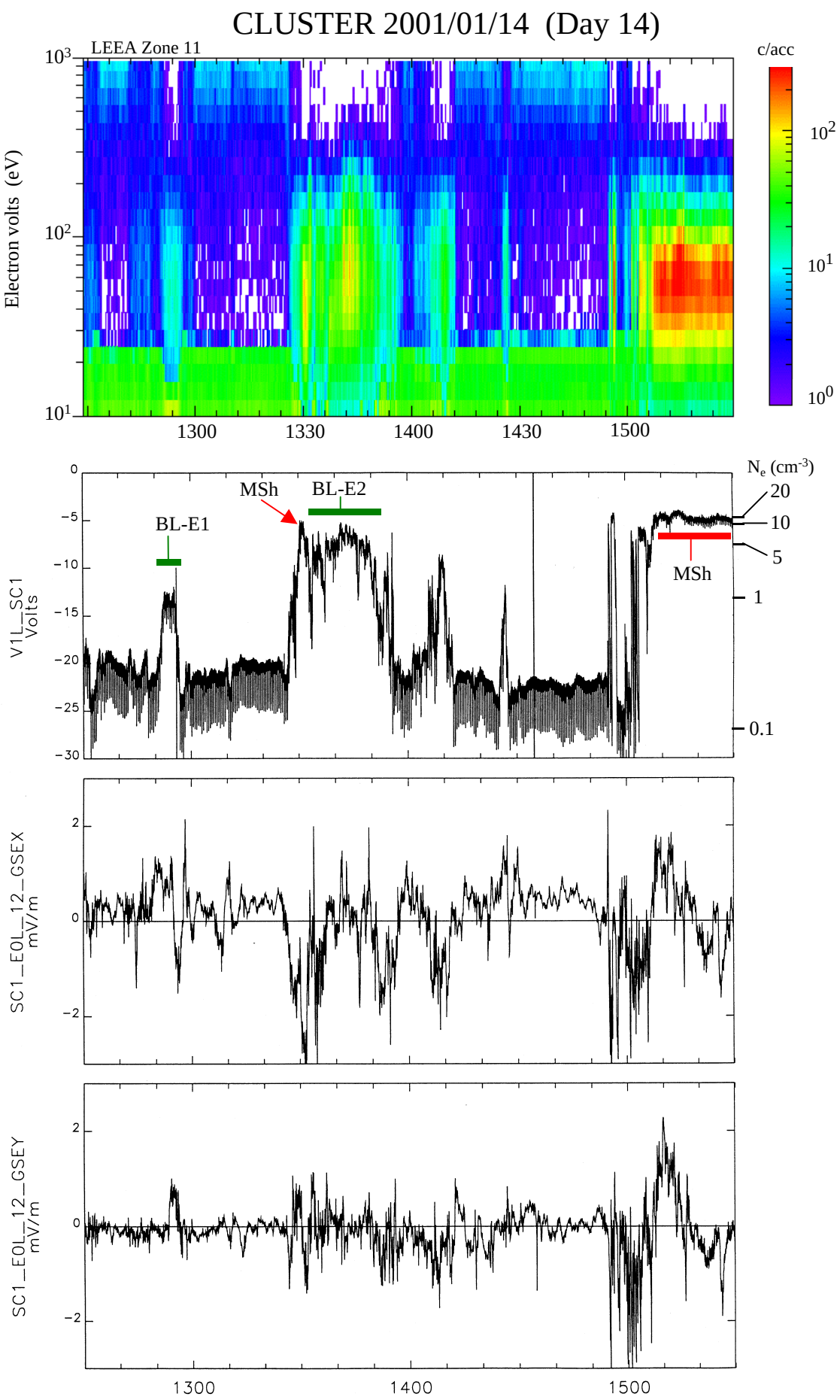
CLUSTER 2001/01/14 (Day 14)
LEEA Zone 11
c/acc
Electron volts (eV)
10^3
10^2
10^1
10^2
10^1
10^0
1300
1330
1400
1430
1500
N_e (cm^{-3})
20
10
5
1
0.1
MSh
BL-E2
BL-E1
MSh
V1L_SC1
Volts
0
−5
−10
−15
−20
−25
−30
SC1_EOL_12_GSEX
mV/m
SC1_EOL_12_GSEY
mV/m
2
0
−2
1300
1400
1500

Figure 2

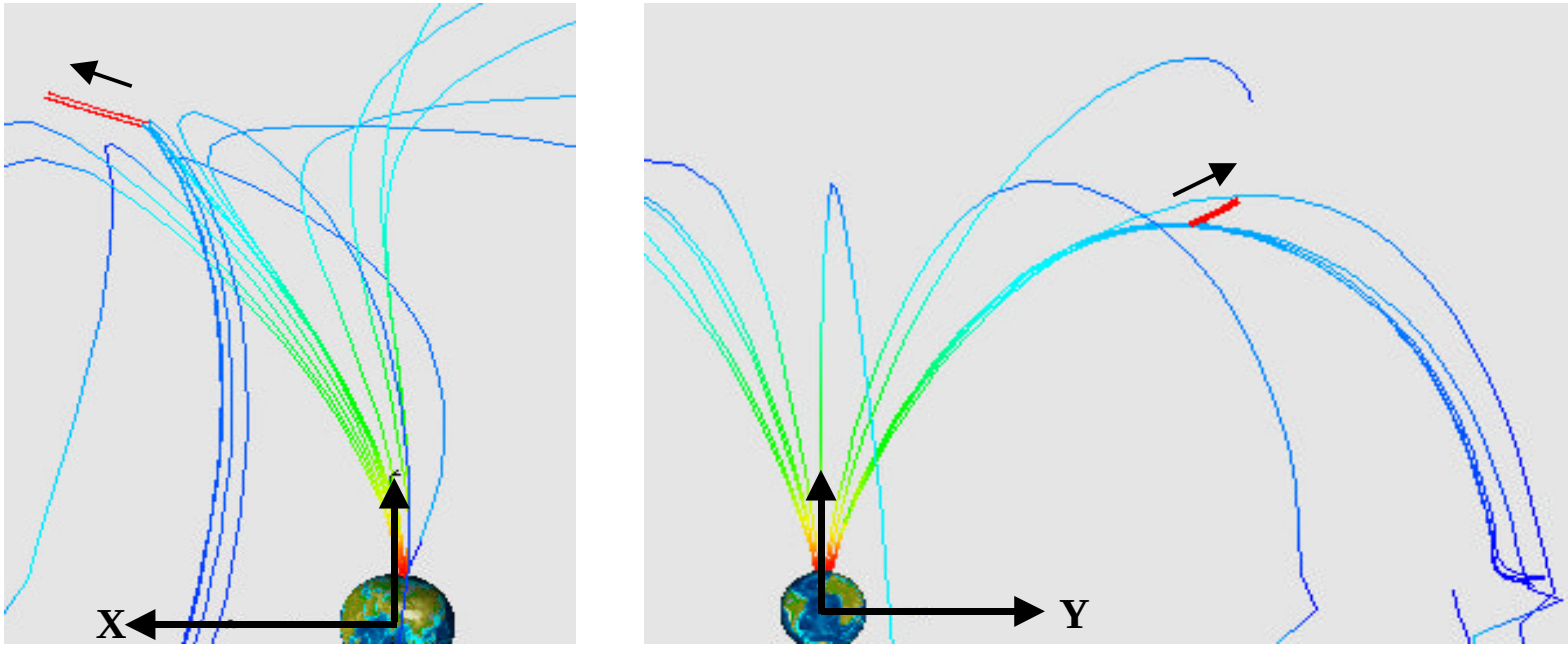

GSE XZ GSE YZ

Figure 1